5th Asia-Pacific Conference on Semiconducting Silicides and Related Materials (APAC-Silicide 2019)
JJAP Conf. Proc. **8**, 011301 (2020) https://doi.org/10.7567/JJAPCP.8.011301

Structural, Optical and AC Conductivity Studies on Polycrystalline-Si/Nanocrystalline-$FeSi_2$ Composite Thin Films

Yuta Saito[1]* and Hiroshi Katsumata[1]

[1]*School of Science and Technology, Meiji University, Kawasaki 214-8571, Japan*

E-mail: katumata@meiji.ac.jp

(Received September 30, 2019)

We investigated an electrical conduction mechanism of Si/$FeSi_2$ composite films by measuring a frequency dependence of AC electrical conductivity. The results were analyzed based upon Jonscher's power law. The hopping conduction obeying the Jonscher's power law was observed for a-Si single films after annealing as well as Si/$FeSi_2$ composite films annealed at 550 and 900℃. From the analysis of XRD, optical absorption, TEM/EDS and AC conductivity, we conclude that the electrical conduction mechanisms in polycrystalline (poly)-Si/β-$FeSi_2$ annealed at 550℃ and poly-Si/α- and β-$FeSi_2$ annealed at 900℃ are due to electron hopping via the conduction band of β-$FeSi_2$ and α-$FeSi_2$ nanocrystals embedded in poly-Si thin films, respectively.

1. Introduction

In recent years, a lot of research efforts in developing all-solid-state secondary battery with high safety and high capacity has been devoted and especially thin-film all-solid-state secondary batteries, which consists of an insulating layer sandwiched between two layers of p-type and n-type inorganic semiconductors, have been proposed [1, 2]. A. Nakazawa proposed a secondary battery with following structures; TiO_2, SnO_2 or ZnO as a n-type layer, NiO or $CuAlO_2$ as a p-type layer, and the charging layer filled with an n-type metal oxide semiconductors of fine particles which were coated with insulating materials [1]. Here we focus on Si/β-$FeSi_2$ composite thin films, which contain nanocrystalline β-$FeSi_2$ particles within Si matrix [3, 4]. Crystalline Si (c-Si) has an indirect band-gap (E_g^{ind}) of 1.12 eV [5], while the amorphous Si (a-Si) has E_g^{ind} values of about 1.4-1.8 eV [6, 7]. β-$FeSi_2$ also exhibits semiconducting properties with a direct band-gap (E_g^{dir}) of 0.87 eV and E_g^{ind} values of 0.765 eV [8, 9]. Therefore, band structure of Si/β-$FeSi_2$ composite thin films becomes similar to the charging layer of proposed secondary battery [1]. Furthermore, the difference between band gaps of Si and β-$FeSi_2$ can be arranged by the degree of crystallinity on Si. From the above points, we believe that Si/β-$FeSi_2$ composite thin films can be used as a charge layer for all-solid-state secondary battery.

However, the electrical conduction mechanism of Si/β-$FeSi_2$ composite films is still unclear. In this study, structural, optical and alternating current (AC) electrical properties of polycrystalline-Si/β-$FeSi_2$ composite thin films were evaluated and the results were compared with those of a-Si single films and the β-$FeSi_2$ single films. The electrical conduction mechanism was discussed based upon the Jonscher's law [10].

2. Experimental procedures

Three Fe chips (4N, 5×5×*t*1 mm, Kojundo Chemical Laboratory Co., Ltd.) were arranged concentrically on a Si target (5N, φ101.6×*t*1 mm, Kojundo Chemical Laboratory Co., Ltd.) and the

Si thin films doped with Fe atoms were deposited on the quartz substrates by RF magnetron co-sputtering (SPF-210H, CANON ANELVA Co., Ltd.) at 0.5 Pa in Ar gas (6N) atmosphere. After the deposition, these samples were annealed in an infrared lamp heating system (Mila-5000, ADVANCE RIKO, Inc.) at 550 or 900°C for 5 hours in a constant Ar gas flow rate of 100 sccm to form Si/β-$FeSi_2$ composite thin films. The a-Si single films and the β-$FeSi_2$ single films were also deposited on the quartz substrates using the Si target as described previously and $FeSi_2$ target (4N, φ101.6×*t*1 mm, Kojundo Chemical Laboratory Co., Ltd.), respectively and then they were annealed under the same above-mentioned conditions for comparison. The film thickness of all samples was around 300 nm. Finally, two rectangular-shaped Al electrodes (area: 16×6.0 mm^2, their distance: 4.5 mm) were deposited on these samples by vacuum thermal evaporation for AC conductivity analysis. Then these samples were alloyed at 450°C for 5 min in Ar gas to form an ohmic contact.

Structural properties of these thin films were evaluated by XRD (SmartLab, Rigaku CO., Ltd.) and TEM/EDS (H-90000NAR, Hitachi High-Technologies Co., Ltd.) analysis and their optical properties were evaluated by optical transmittance and reflectance (V-670 spectrophoto-meter, Jasco CO., Ltd.). Electrical characteristics of these thin films were evaluated by AC conductivity analysis (4284A LCR meter, Agilent Technologies, Inc.) at a DC bias voltage of 0 V and an AC bias voltage of either 0.05 or 1 V as a function of frequency between 100 Hz and 1 MHz.

3. Results and Discussion

Figure 1 shows XRD spectra of annealed samples: (a) $FeSi_2$ single films subjected to annealing at 550°C, (b) Si single films subjected to annealing at 550°C, (c) Si/$FeSi_2$ composite films subjected to annealing at 550°C, and (d) Si/$FeSi_2$ composite films subjected to annealing at 900°C. It was found from Fig. 1(a) that $FeSi_2$ single films subjected to annealing at 550°C shows a polycrystalline β-$FeSi_2$ structure. XRD spectrum of (b) Si single films subjected to annealing at 550°C exhibit an amorphous Si structure, while that of (c) Si/$FeSi_2$ composite films subjected to annealing at 550°C consists of polycrystalline Si and polycrystalline β-$FeSi_2$. The cause of formation of polycrystalline Si at low temperature of 550°C is considered to be due to the metal induced crystallization (MIC) [11, 12]. It should be noted that (d) Si/$FeSi_2$ composite films subjected to annealing at 900°C consist of metallic α-$FeSi_2$, semiconducting β-$FeSi_2$ and poly-Si. We estimated the crystallite sizes, *D* of poly-Si for samples (c) and (d) by Scherrer's equation (*k*=0.9)[13] using the F.W.H.M. values of Si (311) peaks in Figs. 1 (c) and 1 (d), and they were determined to be 3.5 and 7.5 nm, respectively.

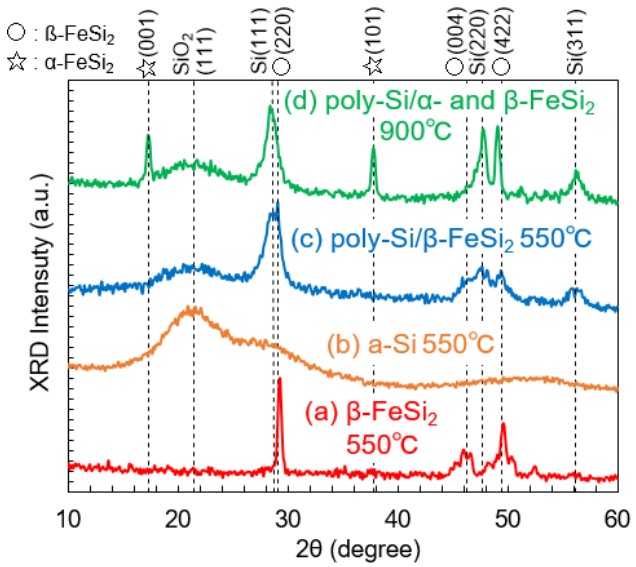

Fig. 1. XRD spectra of annealed samples

Figures 2 (a) and 2 (b) show TEM images of the poly-Si/β-$FeSi_2$ and poly-Si/α- and β-$FeSi_2$ composite thin films formed by annealing at 550 and 900°C, respectively. From the TEM/EDS analysis, the black dots and grey area were identified as $FeSi_2$ and Si, respectively. The particle sizes of $FeSi_2$ dot crystals shown in Figs. 2 (a) and 2(b) were estimated using ImageJ (an open source image processing program) to be 6.8 and 18.8 nm, respectively. Similarly, the distances between $FeSi_2$ particles shown in Figs. 2 (a) and 2(b) were estimated to be 8.95 and 19.5 nm, respectively.

Figure 3 shows optical absorption spectra of annealed samples, which were derived from optical transmittance and reflectance measurements. It is reasonable that the optical absorption coefficient of (d) poly-Si/α- and β-$FeSi_2$ composite films is much smaller than that of (c) poly-Si/β-$FeSi_2$ composite thin films because the reflectance increases with increasing the amount of metallic α-$FeSi_2$. Optical indirect and direct band-gap values (E_g^{ind} and E_g^{dir}) for β-$FeSi_2$ and Si were determined from the optical absorption spectra using Tauc relation [14]. They were E_g^{dir}=0.74 eV for β-$FeSi_2$ single films, E_g^{ind}=1.51 eV for a-Si single films, E_g^{ind}/E_g^{dir}=1.24/0.88 eV for poly-Si/β-$FeSi_2$ composite films, and E_g^{ind}/E_g^{dir}=1.08/0.96 eV for poly-Si/α- and β-$FeSi_2$ composite films. It is known that the band-gap of Si decreases with increasing the degree of crystallinity of Si [15]. As mentioned above, crystallite sizes of poly-Si for poly-Si/β-$FeSi_2$ composite films annealed at 550°C and poly-Si/α- and β-$FeSi_2$ composite films annealed at 900°C were determined to be 3.5 and 7.5 nm, respectively. The difference of the degree of crystallinity is one of the possible origin of the difference of E_g^{ind} for poly-Si. On the other hand, E_g^{dir} for β-$FeSi_2$ depends on chemical composition of Fe/Si as well as the degree of crystallinity of β-$FeSi_2$. The reason for difference in E_g^{dir} for β-$FeSi_2$ is currently unclear. Further investigation on chemical composition of Fe/Si for β-$FeSi_2$ nanocrystals is needed. The summary of analysis results from TEM images and optical absorption spectra is listed in Table I.

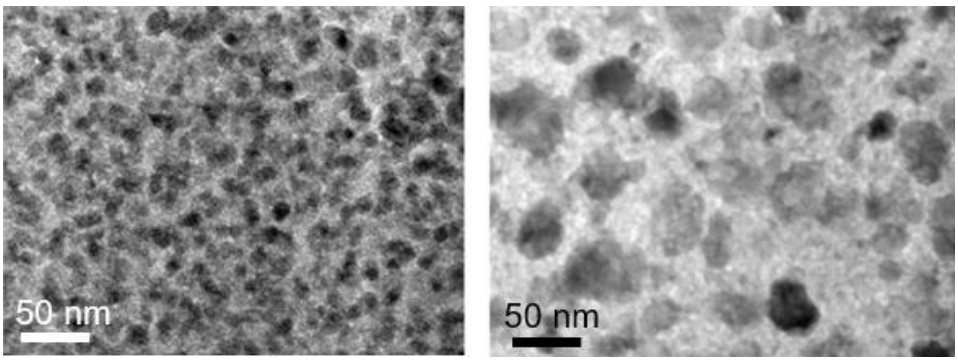

(a) (b)

Fig. 2. TEM images of poly-Si/β-$FeSi_2$ films formed by annealing at 550°C (a) and poly-Si/α- and β-$FeSi_2$ films formed by annealing at 900°C (b)

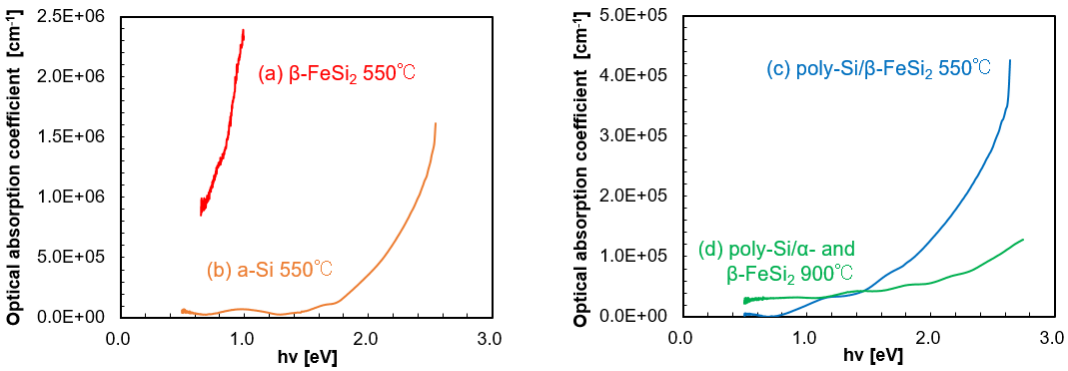

Fig. 3. Optical absorption spectra of annealed samples: (a) β-$FeSi_2$ single films subjected to annealing at 550°C, (b) a-Si single films subjected to annealing at 550°C, (c) poly-Si/β-$FeSi_2$ films formed by annealing at 550°C, and (d) poly-Si/α- and β-$FeSi_2$ films formed by annealing at 900°C.

Table I. Summary of analysis results from TEM images and optical absorption spectra

Sample	The particle size of $FeSi_2$ [nm]	The distance between $FeSi_2$ particles [nm]	Optical band gap [eV]
a-Si 550℃	-	-	1.51
β-$FeSi_2$ 550℃	-	-	0.74
poly-Si/β-$FeSi_2$ 550℃	6.8	8.9	1.24 / 0.87
poly-Si/α- and β-$FeSi_2$ 900℃	18.8	19.5	1.08 / 0.96

Figure 4(a) shows the angular frequency dependence of the electrical AC conductivity for various films after annealing. It is known that the AC electrical conductivity of a substance exhibiting hopping conduction obeys Jonscher's power law and it is expressed as Eq. (1) [10, 16, 17],

$$\sigma_{ac} = A\omega^s, \omega = 2\pi f \qquad (1)$$

where A is a constant dependent on temperature, ω is the angular frequency, f is frequency and s is the frequency exponent ($0 < s \leq 1$). Hopping conduction was observed for three types of films; a-Si single films after annealing at 550℃, poly-Si/β-$FeSi_2$ composite films formed by annealing at 550℃ and poly-Si/α- and β-$FeSi_2$ composite films formed by annealing at 900℃. It has been suggested that the electric conduction mechanism of amorphous materials is mainly due to hopping conduction [18, 19]. Therefore, it is natural that a-Si single films after annealing show hopping conduction in a wide range of angular frequency. On the other hand, poly-Si/β-$FeSi_2$ and poly-Si/α- and β-$FeSi_2$ composite films show hopping conduction only at higher angular frequencies and in a wide range of angular frequency, respectively. The discussion of these electrical conduction mechanisms will be described later.

The polaron binding energy, W_m and the lower bound cut off to hopping distance, R_{min} were calculated using Eqs. (2) [16] and (3) [17], respectively,

$$s = 1 - \frac{6kT}{W_m} \qquad (2)$$

$$R_{min} = \frac{ne^2}{\pi\varepsilon\varepsilon_0 W_m} \qquad (3)$$

where k is the Boltzmann constant, T is the temperature, n=1, 2 for single and bi-polarons, e is the elementary charge, and ε and ε_0 is the relative dielectric constant of a material and dielectric constant of a vacuum, respectively. Here, the value of ε was calculated from the capacitance value of each sample, which was measured by AC conductivity analysis as a function of frequency. The values of R_{min} were obtained assuming n=2 and they are shown in Fig. 4(b) as a function of angular frequency. Curve fitting results using Eqs. (1)-(3) are summarized in Table II.

The difference between bottom of conduction bands of crystalline-Si (electron affinity, χ =4.05 eV) [20] and β-$FeSi_2$ (χ =4.71 eV) [20] can be estimated to be 0.66 eV, which almost agrees well with W_m value (0.64 eV) of poly-Si/β-$FeSi_2$ composite films. In addition, as shown in Table I, the distance between $FeSi_2$ particles for poly-Si/β-$FeSi_2$ composite films was 8.9 nm, which is of the same order of magnitude as R_{min} value (3.3 nm) of poly-Si/β-$FeSi_2$ composite films. For the above reasons, it is suggested that the electrical conduction in poly-Si/β-$FeSi_2$ composite films is due to electron hopping via the conduction band of β-$FeSi_2$. Similarly, the difference between bottom of conduction bands of crystalline-Si (χ =4.05 eV) [20] and α-$FeSi_2$ (work function=5.3-5.5 eV) [21]

can be estimated to be 1.43-1.45 eV, which is roughly close to W_m value (1.88 eV) of poly-Si/α- and β-$FeSi_2$ composite films. Work function of 5.3-5.5 eV on α-$FeSi_2$ is larger than electron affinity of 4.71 eV on β-$FeSi_2$. Therefore, it is suggested that the electrical conduction in poly-Si/α- and β-$FeSi_2$ composite films is due to electron hopping via the conduction band of α-$FeSi_2$. The distance between $FeSi_2$ particles for poly-Si/α- and β-$FeSi_2$ composite films was 19.5 nm, which is of the different order of magnitude as R_{min} value (2.3 nm) of poly-Si/α- and β-$FeSi_2$ composite films. This reason is currently unclear because poly-Si/α- and β-$FeSi_2$ composite films consist of mixed phase of α- and β-$FeSi_2$. We need to form and evaluate poly-Si/α-$FeSi_2$ single phase composite films to clarify it.

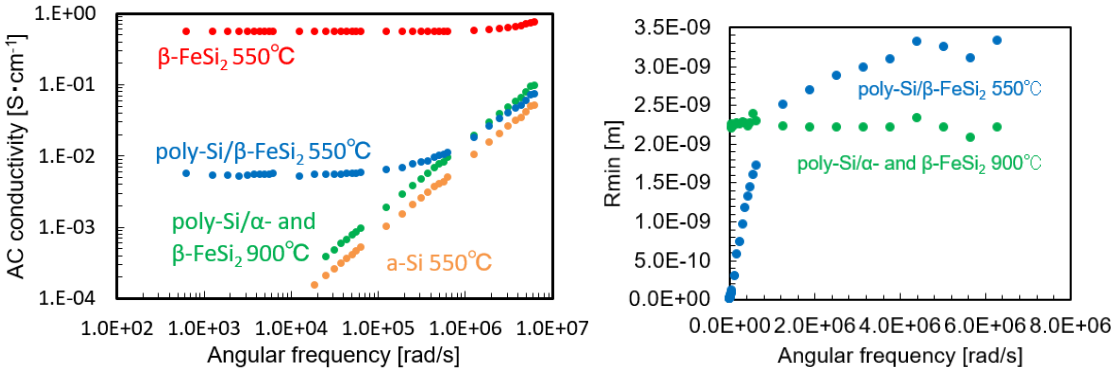

Fig. 4. (a) AC conductivity and (b) hopping distance R_{min} as a function of angular frequency

Table II. Summary of AC conductivity analysis

Sample	annealing	s	W_m [eV]	R_{min} [nm] @ 4.40×10^6 [rad/s]
a-Si single films	550℃	1.00	∞	N/A
Si/$FeSi_2$ composite films	550℃	0.762	0.64	3.3
	900℃	0.909	1.88	2.3

4. Conclusion

XRD and optical absorption spectra of β-$FeSi_2$ single films showed a polycrystalline β-$FeSi_2$ structure with the E_g^{dir} value of 0.74 eV, while those of a-Si single films exhibited an amorphous Si structure with the E_g^{ind} value of 1.51 eV. We found that the poly-Si/β-$FeSi_2$ composite films annealed at 550℃ consist of polycrystalline Si (E_g^{ind} = 1.24 eV) and nanocrystalline β-$FeSi_2$ (E_g^{dir} = 0.87 eV, the particle size is 6.8 nm). Similarly, we found that the poly-Si/α- and β-$FeSi_2$ annealed at 900℃ composite films consist of nanocrystalline α-$FeSi_2$ and β-$FeSi_2$ (E_g^{dir} = 0.96 eV, the particle size is 18.8 nm) and polycrystalline Si (E_g^{ind} = 1.08 eV).

We investigated an electrical conduction mechanism of Si/$FeSi_2$ composite films by measuring a frequency dependence of AC electrical conductivity. The results were analyzed based upon Jonscher's power law and the three parameters, s, W_m and R_{min} were determined by fitting the calculated values to the experimental data. The hopping conduction obeying the Jonscher's power law was observed for a-Si single films after annealing as well as Si/$FeSi_2$ composite films annealed at 550 and 900 ℃. The hopping conduction in a-Si films has been reported so far. From the result of comparison between W_m values and the band diagram of Si/$FeSi_2$ as well as between R_{min} values and the distance between $FeSi_2$ particles, we conclude that the electrical conduction mechanisms in poly-

Si/β-$FeSi_2$ and poly-Si/α- and β-$FeSi_2$ composite films are due to electron hopping via the conduction band of β-$FeSi_2$ and α-$FeSi_2$ nanocrystals embedded in poly-Si films, respectively.

References

[1] Akira Nakazawa, US patent, US9887441B2 (2018).
[2] Atsuya Sasaki, Akito Sasaki, Hideaki Hirabayashi, Shuichi Saito, Katsuaki Aoki, Yoshinori Kataoka, Koji Suzuki, Hidehiko Yabuhara, Takahiro Ito, and Shigeyuki Takagi, Jpn. J. Appl. Phys., **57**, 041201 (2018).
[3] K. Okajima, H. Yamatsugu, C. Wen, M. Sudoh, and K. Yamada, Thin Solid Films, **381**, 267 (2001).
[4] M. Sawata and H. Katsumata, Extended abstract of International Thin Films Conference TACT 2015, P-C25-0191 (2015).
[5] S. M. Sze "Physics of Semiconductor Devices", pp. 12-15 (1981).
[6] N. M. Ravindra, C. Ance, S. P. Coulibaly, F. De Chelle, J. M. Berger, J. P. Ferraton, and A. Donnadieu, Infrared Phys., **23**, 99 (1983).
[7] Barbara Swatowska, Stanislawa Kluska, Maria Jurzecka-Szymacha, Tomasz Stapinski, and Katarzyna Tkacz-Smiech, Appl. Surf. Sci., **371**, 91 (2016).
[8] A. B. Filonov, V. E. Borisenko, W. Henrion, and H. Lange, J. Luminescence, **80**, 479 (1999).
[9] Ken-ichiro Takakura, Noriyoshi Hiroi, Takashi Suemasu, Shigefusa F. Chichibu and Fumio Hasegawa, Appl. Phys. Lett., **80**, 556 (2002).
[10] A. K. Jonscher, Nature, **267**, 673 (1977).
[11] Soo Young Yoon, Seong Jin Park, Kyung Ho Kim, and Jim Jang, Thin Solid Films, **383**, 34 (2001).
[12] W. Knaepen, C. Detavernier, R. L. Van Meirhaeghe, J. Jordan Sweet, and C. Lavoie, Thin Solid Films, **516**, 4946 (2008).
[13] Hosein Kafashan, J. Electron. Mater., **48**, 2 (2019).
[14] J. Tauc and A. Menth, J. Non-Crystalline Solids, **8-10**, 569 (1972).
[15] X. Xu, J. Yang, A. Banerjee, and S. Guha, K. Vasanth, and S. Wagner, Appl. Phys. Lett., **67**, 16 (1995).
[16] R. Dridi, I. Saafi, A. Mhamdi, A. Yumak, M. Haj Lakhdar, A. Amlouk, K. Boubaker, and M. Amlouk, J. Alloys and Compd., **634**, 179 (2015).
[17] Arvind Sharma, Amit Kumar, and Neeraj Mehta, Measurement, **75**, 69 (2015).
[18] Abdullah Yidiz, Necmi Serin, Tülay Serin, and Mehmet Kasap, Jpn. J. Appl. Phys., **48** 111203 (2009).
[19] Yanping Yao, Baoxue Bo, and Chunling Liu, Curr. Appl. Phys., **18**, 1492 (2018).
[20] Xin-Yao Zou, Modern Phys. Lett. B, **31**, 1740026 (2017).
[21] Goutam Kumar Dalapati, Cheng Cheh Tan, Saeid Masudy-Panah, Hui Ru Tan, and Dongzhi Chi, Mater. Lett., **159,** 455 (2015).